JTTEE5 11:195-205

Calibration of a Two-Color Imaging Pyrometer and Its Use for Particle Measurements in Controlled Air Plasma Spray Experiments

S.P. Mates, D. Basak, F.S. Biancaniello, S.D. Ridder, and J. Geist

(Submitted 14 November 2000; in revised form 19 January 2001)

Advances in digital imaging technology have enabled the development of sensors that can measure the temperature and velocity of individual thermal spray particles over a large volume of the spray plume simultaneously using imaging pyrometry (IP) and particle streak velocimetry (PSV). This paper describes calibration, uncertainty analysis, and particle measurements with a commercial IP-PSV particle sensor designed for measuring particles in an air plasma spray (APS) process. Yttria-stabilized zirconia (YSZ) and molybdenum powders were sprayed in the experiments. An energy balance model of the spray torch was used to manipulate the average particle velocity and temperature in desired ways to test the response of the sensor to changes in the spray characteristics. Time-resolved particle data were obtained by averaging particle streaks in each successive image acquired by the sensor. Frame average particle velocity and temperature were found to fluctuate by 10% during 6 s acquisition periods. These fluctuations, caused by some combination of arc instability, turbulence, and unsteady powder feeding, contribute substantially to the overall particle variability in the spray plume.

Keywords air plasma spray, calibration control, imaging pyrometry, particle sensor

1. Introduction

Non-intrusive in-flight measurement of thermal spray particle velocity, temperature, and size has become a useful tool in thermal spray technology. Particle sensors are used to verify proper spray torch operation for industrial quality control purposes,[1] to investigate relationships between processing conditions and coating properties,[2-4] and to supply data to validate computational models of thermal spray processes.[5] Sensors have also been used to achieve closed-loop control of thermal plasma spraying.[6] Although competition in the area of industrial quality control has arisen with simpler sensors that measure ensemble properties of the spray plume rather than individual particles,[7,8] individual particle sensors are the most flexible and powerful diagnostic tools for thermal sprays.

The velocity of thermal spray particles has been measured using several techniques, including laser Doppler velocimetry (LDV),[9] particle streak velocimetry (PSV),[10] phase Doppler interferometry (PDI),[11] and others.[1] Thermal spray particle temperature is most often measured by two-color pyrometry, although spectroscopic techniques have also been used.[12] With two-color pyrometry, the temperature of a particle is determined from the ratio of the thermal radiation it emits in two separate spectral regions. The spectral regions are carefully chosen to provide high sensitivity and low interference from nonthermal background light. Two-color pyrometry has the advantage of being independent of the size of the particle, its position in the field of view, and its emissivity, provided that it does not vary over the spectral regions of interest. Its main drawback is that the emissivity of spray particles is unknown and may vary with wavelength, inviting the possibility of large systematic errors in particle temperature. Despite this possible error, however, two-color pyrometry offers considerable advantages for measuring thermal spray particle temperatures in flight.

The typical two-color pyrometer used in thermal sprays collects light from a small volume in the particle-laden spray plume.[1,11,13] Thermal emission is collected from individual particles passing through this volume at two separate wavelengths. Particle temperature is determined from the ratio of the detector signals using a calibration curve. To obtain an average particle temperature, individual particle measurements are accumulated at a given location over a period of time. The entire spray plume can be mapped in three dimensions by translating the measurement volume relative to the torch.

A new implementation of two-color pyrometry for thermal sprays involves the use of an electronically shuttered charge-coupled device (CCD) camera to image bright particle streaks over a large volume of the spray plume simultaneously.[14,15] The principles of two-color imaging pyrometry (IP) are identical to the small volume approach, except that the optical filtering is done on an image basis. The advantage of imaging pyrometry is that the sensor need not be scanned to measure the entire particle stream because it measures particles across the entire width of the plume at once. In addition to measuring particle temperatures, the device measures particle velocities by PSV, and particle sizes can be inferred from streak widths.[15] Histograms of particle properties can be displayed in real time (>1 Hz) so that spray parameters can be tuned to achieve desired particle velocity and temperature distributions rapidly. This technique can

S.P. Mates, D. Basak, F.S. Biancaniello, and **S.D. Ridder,** Metallurgy Division, National Institute of Standards and Technology, Gaithersburg, MD 20899-8556; and **J. Geist,** Sequoyah Technologies, Gaithersburg, MD. Contact e-mail: steven.mates@nist.gov.

also indicate how the average particle temperature, velocity, and flux change with time due to the various sources of unsteadiness in the plasma spray process, including arc root motion, turbulence, and oscillations in the powder feed rate to the torch.

This paper describes the calibration and use of a two-color IP-PSV (Stratonics, Inc., Laguna Hills, CA*).[14] The instrument is used to measure particle temperatures and velocities produced by a model SG-100 (Praxair, Danbury, CT) air plasma spray (APS) torch. Particle measurements are reported for commercial yttria-stabilized zirconia (YSZ) and molybdenum powders sprayed with a set of torch parameter settings selected to manipulate particle velocity and temperature over the widest possible range. The parameter matrix was designed with the aid of a one-dimensional, steady-state energy balance model of the spray torch that describes how the torch parameters influence the acceleration and heating of individual spray particles. Average particle velocity, temperature, and flux are also presented as a function of time, revealing the effect of the various sources of unsteadiness in this thermal spray process on the particle stream.

*The use of commercial products or tradenames is for identification purposes only. Such identification is not intended to imply endorsement or evaluation of the relative merits of these items by NIST.

Nomenclature

A_e	torch nozzle exit area (m^2)
A_p	particle surface area (m^2)
D	particle diameter (μm)
h	heat transfer coefficient (W/m^2K)
H	specific enthalpy (J/kg)
I	current (A)
i_r	intensity ratio
k	thermal conductivity (W/mK)
$\dot{m}$	mass flow (kg/s)
P	planck function
Pr	prandtl number ($\mu c_p/k$)
Q	CCD spectral responsivity
q''	heat transfer rate (W/m^2)
Re	Reynolds number $[\rho_g(U_g - U_p)D/\mu_g]$
S	spectral intensity
T	temperature (K)
t	time (s)
U	velocity (m/s)
V	voltage (V)

Subscripts

[1,0]	number average size
e	torch exit
g	gas or plasma
i	torch inlet
L	long wavelength band
m	melting point
p	particle
S	short wavelength band
T	temperature
V	velocity
v,50	mass median size

Greek Symbols

β	fit coefficient
ε	emissivity
η	torch thermal efficiency
λ	wavelength (nm)
ρ	density (kg/m^3)
σ	standard deviation
τ	filter transmission

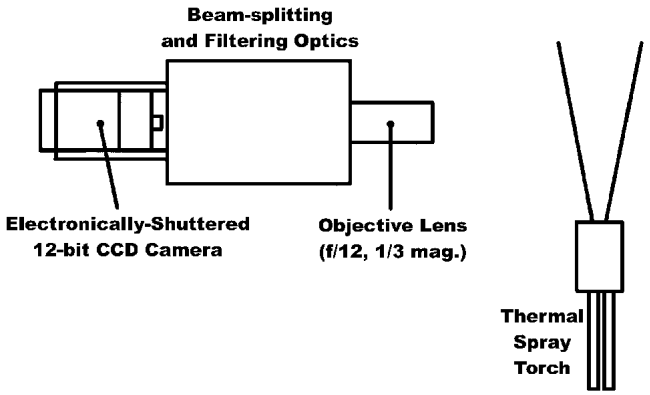

Fig. 1 Schematic of the IP-PSV

2. Description and Calibration of the IP-PSV Sensor

2.1 Sensor Description and Operation

A schematic of the IP-PSV thermal spray sensor is shown in Fig. 1. It consists of a collecting lens, beam-splitting and filtering optics, and an electronically shuttered CCD camera. The sensor images the spray plume and splits the single image into two identical images, which are then band-pass filtered in separate spectral regions and focused onto adjacent halves of the CCD array. Figure 2 shows a sample (dual) image of molybdenum particle streaks. The sensor described here uses a commercially available 12-bit 640 × 480 pixel CCD camera with a minimum exposure time of 50 ns. Typical exposure times range from 5 to 20 μs, depending on particle velocity. The CCD array is Peltier-cooled to limit drift, noise, and dark current. It senses radiation between approximately 500 and 1000 nm. At the overall magnification factor of the optics, each pixel corresponds to 32 μm of real space. The CCD fill factor is nearly 100% owing to special hardware modifications, which eliminate the interpixel dark space according to the manufacturer (Optikon Kitchener, ON, Canada).

As described by several authors,[1,11,13] the choice of spectral bandwidths used to measure the two-color particle intensity signal affects temperature sensitivity and the possibility for signal contamination from scattered plasma light. The signal-to-noise ratio must also be considered when selecting spectral bandwidths, because they determine what fraction of the available spectral radiation is sampled. Because the spray particles are small and pass quickly through the measurement volume, only a limited amount of radiation is available to measure. For good sensitivity at temperatures above 3000 K, and to maximize the available radiation signal, the IP-PSV uses a short wavelength

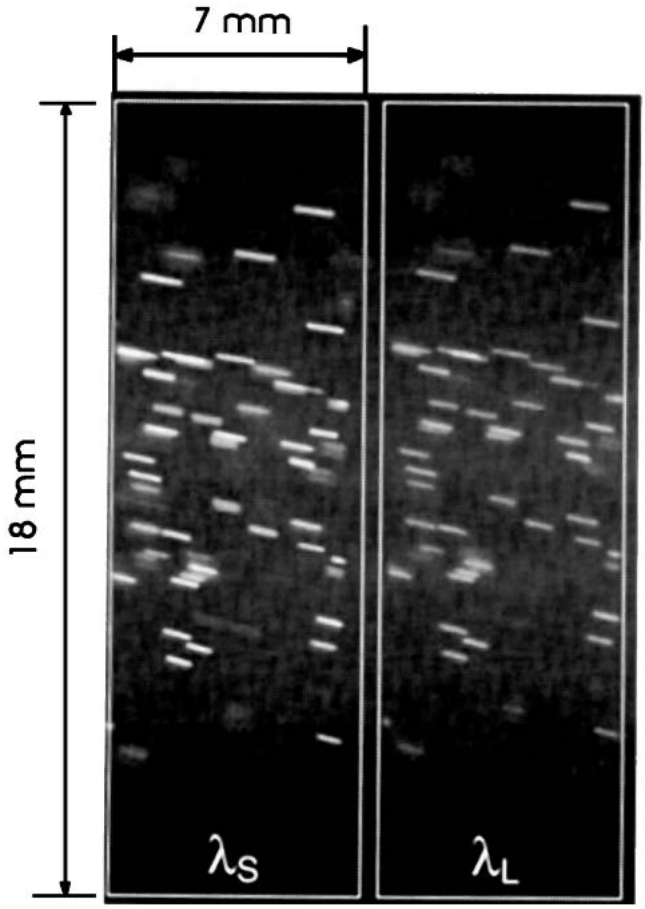

Fig. 2 Sample dual image of hot molybdenum particle streaks; particles are moving left to right

band covering 600 nm (λ_1) to 750 nm (λ_2), and a long wavelength band covering 750 to 1000 nm (λ_3).

In a single measurement, up to 300 images of particle streaks can be acquired at a rate of 24 frames/s. Images are stored in PC memory for subsequent processing. Analysis software scans each image to identify individual particle streaks and compute velocity and temperature. Particle velocity is determined by dividing the streak length by the exposure time. Particle temperature is determined from the streak intensity ratio using a fit to calibration data. Individual streak intensities are computed by integrating pixel intensities over a region encompassing the entire streak plus a small amount of background. This technique maximizes the signal-to-noise ratio and minimizes errors due to optical aberrations and focus. Several criteria are applied to eliminate invalid streak data. Invalid data include streaks that are badly out of focus, partially out of the field of view, or coincident with other streaks, such that their intensities are difficult to distinguish. Badly out-of-focus streaks are eliminated using an empirically determined minimum acceptable length-to-width ratio. A minimum streak intensity threshold is applied to eliminate streaks with an unacceptably small signal-to-noise ratio. The uncertainty in the measured streak intensities falls between ±0.4% and 2%, depending on the intensity level, based on a 2σ noise level of ±4 counts per pixel and a resolution limit of ±0.5 counts per pixel.

2.2 Temperature Calibration Procedure

A model of the IP-PSV sensor that relates the measured intensity ratio to the absolute temperature of the target can be defined using nominal functions for the spectral responsivity of the CCD, $Q(\lambda)$, and the filter transmissions $\tau(\lambda)$:

$$i_r = \frac{\int_{\lambda_2}^{\lambda_3} P(\lambda, T) \cdot \varepsilon(\lambda, T) \cdot \tau(\lambda) \cdot Q(\lambda) d\lambda}{\int_{\lambda_1}^{\lambda_2} P(\lambda, T) \cdot \varepsilon(\lambda, T) \cdot \tau(\lambda) \cdot Q(\lambda) d\lambda} \quad \text{(Eq 1)}$$

The graybody assumption eliminates emissivity, ε. Ideally, particle temperature could be determined from the intensity ratio directly from this model. However, calibration is needed because $Q(\lambda)$ and $\tau(\lambda)$ are not known precisely. The developers of the IP-PSV provided calibration data between 1173 and 2848 K obtained using a tungsten strip lamp, the absolute temperature of which was measured with a spectrometer and the emissivity effects of which were corrected for using literature values for tungsten.[14] However, because particle temperatures in plasma spray plumes can exceed 3000 K, particularly for high melting point materials such as molybdenum (T_m = 2883 K) and YSZ (T_m = 2950 K), additional calibration data beyond 2848 K were sought.

The calibrated range of the sensor was extended using a unique nonintrusive temperature measurement facility in the Sub-Second Thermophysics Laboratory (SSTL) at the National Institute of Standards and Technology (NIST). The facility was originally designed to measure the melting temperature of metals and alloys subject to fast heating rates.[16] By providing an optically accessible target at a known, selectable absolute temperature up to the melting point of tungsten (3693 K), this facility served as an excellent variable temperature calibration source for the IP-PSV. A sketch of the calibration experiment is shown in Fig. 3. Metal samples, consisting of small (1.6 mm diameter) rods, are placed in an argon-filled, optically accessible chamber and pulse-heated with an electric current to a preselected temperature. Upon reaching a stable temperature, the samples' radiance temperature is measured at 651 nm using a single-color pyrometer and its normal spectral emissivity is measured at 633 nm by laser polarimetry.[17] Plank's law is then used to determine the samples' absolute temperature from these measurements to within ±8 K.[18] Calibration data, consisting of intensity ratio and corresponding absolute temperature measurements, were acquired using tungsten and molybdenum samples at temperatures between 1541 and 3654 K.

As with most polished metals, the emissivity of molybdenum and tungsten decreases slightly over the wavelength range of interest.[19] Thus, the calibration sources are not truly gray, so that the intensity ratios measured by the IP-PSV deviate from what would have been measured if an ideal calibration source, such as a blackbody, were used instead. To avoid passing this systematic error on to the particle measurements, a fiber-optic spectrometer (FOS) was used to simultaneously measure the spectral shape of the radiation emitted by the metal rods to correct the calibration for non-graybody effects. The correction was determined by integrating the spectral data [$S(\lambda)$], weighted by $Q(\lambda)$, over the wavelength bands of the IP-PSV, and comparing the resulting intensity ratio to the equivalent ratio obtained with

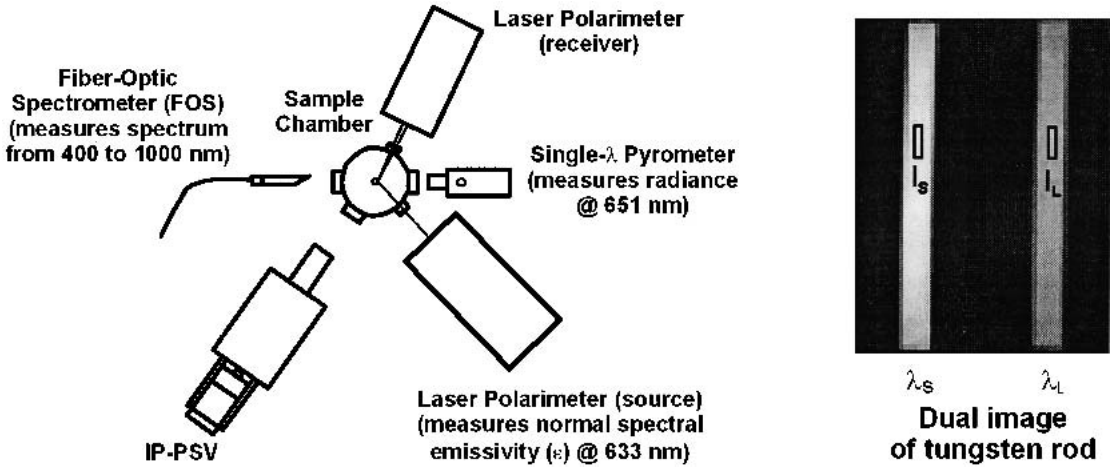

Fig. 3 Schematic of the measurement facility in the NIST's Sub-Second Thermophysics Laboratory used to calibrate the IP-PSV for temperature

the Planck function. The quotient of these ratios is a measure of how the emissivity of the calibration source affects its radiant emission as seen by the IP-PSV:

$$C(T) = \frac{\int_{\lambda_2}^{\lambda_3} S(\lambda, T)Q(\lambda)d\lambda / \int_{\lambda_1}^{\lambda_2} S(\lambda, T)Q(\lambda)d\lambda}{\int_{\lambda_2}^{\lambda_3} P(\lambda, T)Q(\lambda)d\lambda / \int_{\lambda_1}^{\lambda_2} P(\lambda, T)Q(\lambda)d\lambda} \quad \text{(Eq 2)}$$

The correction factor $C(T)$ was applied point by point to obtain an effective "graybody" calibration for the IP-PSV. Some uncertainty exists in $C(T)$ because of uncertainties in $Q(\lambda)$ and the filter cutoff wavelengths.

Raw and corrected intensity ratio data are plotted in Fig. 4 against inverse absolute temperature. The emissivity-corrected data differ from the uncorrected data by approximately 9% for both the tungsten and molybdenum samples, which have nearly the same emissivity characteristics. In terms of temperature, the graybody assumption introduces a systematic error of 50 K at 1600 K and almost 300 K at 3654 K. If uncorrected, this error would be passed on to the measured (graybody) particle temperature. Also included in Fig. 4 are the tungsten lamp calibration data supplied by the instrument developer.[14] Their calibration data, which are also emissivity-corrected, agree well with the present emissivity-corrected calibration data, providing additional confidence in both calibration techniques.

The equation for temperature is obtained by fitting the emissivity-corrected calibration data using the following function:

$$T = \frac{\beta_1}{\ln(i_r) + \beta_0} \quad \text{(Eq 3)}$$

The fit coefficients are $\beta_0 = 2.1106$ and $\beta_1 = 4160.9$ for the emissivity-corrected data. The standardized residuals for the fit, plotted in Fig. 5, are randomly scattered, indicating that a consistently good fit was achieved over the temperature range considered. The 95% confidence intervals for temperature predictions with the calibration equation, based on the assumption

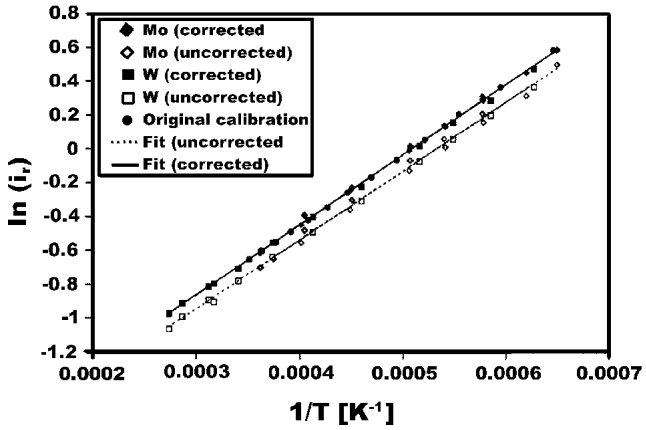

Fig. 4 Temperature calibration data and fits with and without correcting for emissivity. The original calibration data from the instrument developer[14] were obtained using a tungsten lamp.

of randomly distributed measurement errors,[20] are estimated at 1% at 1500 K and 2.5% at 3500 K.

2.3 Uncertainty on Individual Particle Temperature and Velocity

The uncertainty on an individual particle temperature, considering only the accuracy of the streak intensity measurement, is estimated at between 1% and 3%, depending on the brightness and temperature of the particle. This estimate assumes that the streak intensity represents only radiation caused by thermal emission from the particle. At the typical measurement distance (90 to 100 mm), the contribution of reflected plasma light becomes negligible for particles above about 1800 K.[21] The uncertainty generally increases with temperature because the intensity ratio becomes less sensitive to changes in temperature according to the Planck function. This is partially offset by the increase in signal-to-noise ratio at higher temperatures. Together with the calibration uncertainty, the overall uncertainty in particle temperature ranges from 1.5-4% based on random errors alone.

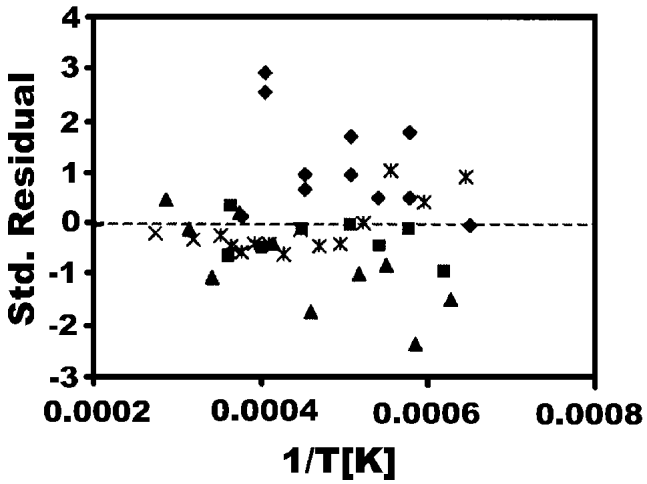

Fig. 5 Standardized residuals for calibration fit to emissivity corrected data. Different symbols indicate different materials, calibration techniques, or experiments.

If the spray particles deviate from graybody behavior, potentially significant systematic errors in temperature may occur. The calibration experiments indicate that this error can be more than 100 K for nonoxidized molybdenum or tungsten when using the IP-PSV. However, without reliable emissivity data for thermal spray particles, whose emissivity characteristics may change significantly because of in-flight oxidation, corrections to the graybody assumption for particles are not presently feasible.

Uncertainties involved in measuring the magnitude of the particle velocity arise mainly from estimating the length of the streak. Uncertainties in streak length arise because of optical aberrations, focus, and particle trajectory. Optical aberrations smear the streak boundary, making its length ambiguous by one or two pixels, yielding an uncertainty of 5-10% for a streak 20 pixels long. Lengthening the streaks by increasing the exposure time can reduce this uncertainty. The tradeoff is an increased number of coincident streaks and a higher data rejection rate. A similar uncertainty exists for streaks that are slightly out of focus. A small uncertainty (less than 1%) occurs because the particle stream diverges by approximately 5°, causing some streaks to appear shorter by a factor equal to the cosine of their angle away from the image plane.

Because particle size is proportional to the width of its streak, size information can, in principle, be extracted from the data. However, because streak width is affected by focus as well as optical aberration, additional information is needed to accurately determine particle size. For example, particle size could be estimated using the particle size distribution of the feedstock powder as a rough calibration.[15] In this paper, however, particle size measurements were not attempted.

3. Air Plasma Spray Experiments

The IP-PSV was tested in a series of spray experiments involving a Praxair SG-100 plasma spray torch in which the average particle velocity and temperature were varied over the widest practical range by changing the arc current and the plasma gas flow rate. Two different spray powders, molybdenum and YSZ, were included to further expand the range of particle velocities and temperatures. A method for manipulating torch parameters to vary the average particle velocity and temperature in desired ways was developed using a one-dimensional energy balance model of the plasma torch and models for particle acceleration and heating within the plasma jet.

3.1 Method for Selecting Torch Parameters to Vary Particle Velocity and Temperature

The equations describing the acceleration and heating of individual thermal spray particles in a plasma flow were summarized by Pfender:[23]

$$\frac{dU_p}{dt} = \frac{3\pi}{4\rho_p D}\rho_g (U_g - U_p)^2 \quad \text{(Eq 4)}$$

$$q'' = hA_p (T_g - T_p) \quad \text{(Eq 5)}$$

$$h = \frac{k}{D}(2 + \mathrm{Re}^{0.5}\mathrm{Pr}^{0.33}) \quad \text{(Eq 6)}$$

To predict U_p and T_p at a given location, these equations can be integrated over the particles' flight path through a specified plasma flow field using advanced computational tools.[5] However, to develop basic insight as to how the torch parameters affect the average velocity and temperature of the spray particles, simplifying assumptions can be made.

The first assumption involves the averaged effects of turbulent mixing on the acceleration and heating of the spray particles. Turbulent mixing of the plasma jet proceeds quickly, as shown in Fig. 6, because of its low density compared to the surrounding ambient air, which is up to 20 times denser than the plasma. Density ratio effects also contribute to the rapid turbulent mixing of hot high-velocity oxyfuel (HVOF) thermal spray plumes.[24] This active mixing causes the temperature and velocity of the plasma jet to decrease rapidly away from the torch exit.[25] Consequently, much of the momentum and heat transfer from the plasma jet to the particles occurs near the torch exit, where the particles are injected. Thus, an approximate way to establish how torch parameters affect the particles is to determine how these parameters affect the velocity and temperature of the plasma jet near the particle injection location.

Equation 4 reveals that particle acceleration is governed by the dynamic pressure of the plasma, ρU_g^2, while the plasma temperature, T_g, has a first-order effect on particle temperature. Both ρU_g^2 and T_g at the torch exit can be estimated from the torch parameters using a one-dimensional, steady-state, steady-flow energy balance on the plasma gas. A similar two-dimensional method is usually used to specify the boundary conditions for numerical simulations of plasma jets in thermal sprays.[26] The specific enthalpy of the plasma at the torch exit, H_e, equals the specific enthalpy of the cold inlet gas, H_i, plus the energy per unit mass delivered by the arc:

$$H_e = H_i + \frac{\eta VI}{\dot{m}} \quad \text{(Eq 7)}$$

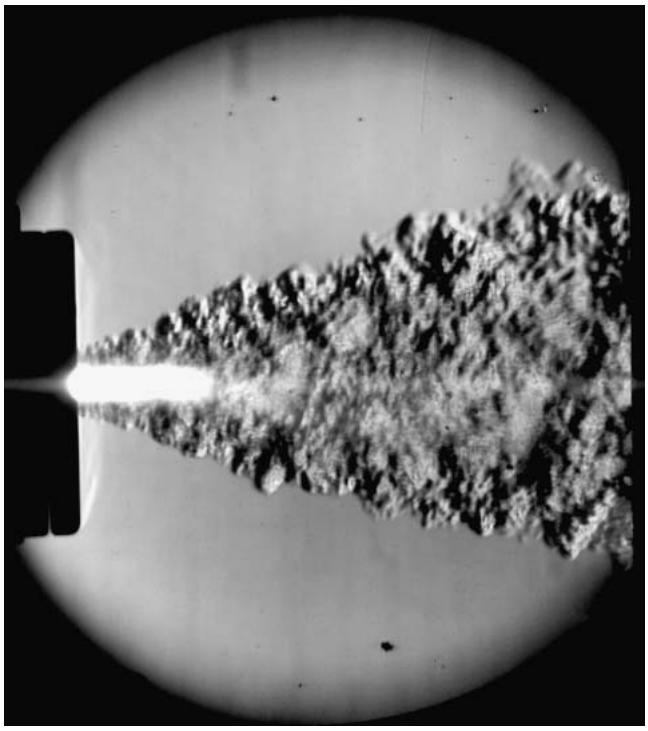

Fig. 6 White-light illuminated, 300 ms exposure schlieren photo showing rapid turbulent mixing of the hot plume produced by an SG-100 plasma spray torch

Table 1 Parameter Matrix to Vary Particle Velocity and Temperature

Condition	Current (A)	Primary Gas Flow (kg/s)
1	380	0.00174
2	550	0.00268
3	650	0.00334
4	500	0.00147
5	700	0.00227
6	860	0.00294
7	850	0.00134
8	950	0.00201
9	1150	0.00281

The remaining plasma properties can be obtained once H_e is established. Thermodynamic and transport property calculations for several single-component plasmas and some mixtures are available in the literature.[27] For simplicity, a single plasma gas (argon) was considered for this study. Finally, conservation of mass is used to estimate the average plasma velocity at the torch exit:

$$U_{g,e} = \frac{\dot{m}}{\rho_g A_e} \quad \text{(Eq 8)}$$

The above method was used to select nine sets of parameter settings, consisting of a current and an argon flow rate, to vary the particle velocity and temperature over a wide range to examine the response of the IP-PSV. These settings, listed in Table 1, include three levels of plasma dynamic pressure and three levels of plasma temperature, as shown in Fig. 7. The specific enthalpy of the plasma was determined at each condition from Eq 7 using the torch current and voltage indicated by the model 3620 control console display and using a thermal efficiency of 60%. The actual torch efficiency varies over a small range with changes in arc current and plasma gas flow rate,[28] and is affected by the condition of the anode and cathode. The powder flow rate was fixed at 15 g/min and the powder carrier gas flow rate (argon) was 0.00015 kg/s (5.6 standard L/min). The plasma torch was outfitted with a # 2083-730 anode, a #2083-720 cathode, and #112 gas injector ring. Powder was injected through the upper port at a forward angle of 10° using Model 1270 powder feeders (Praxair).

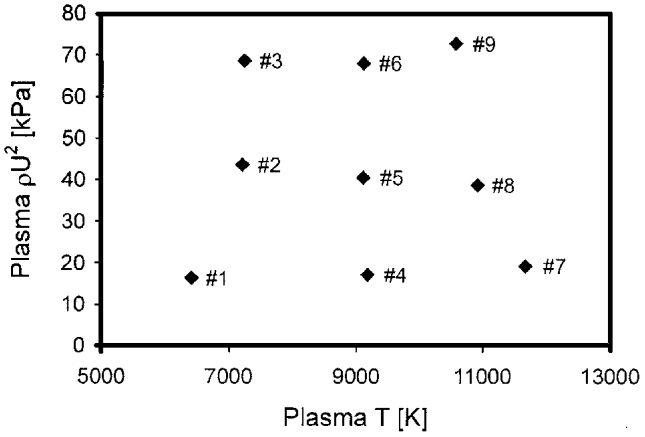

Fig. 7 Plasma dynamic pressure and temperature at the spray torch exit predicted from the energy balance for parameter settings 1-9

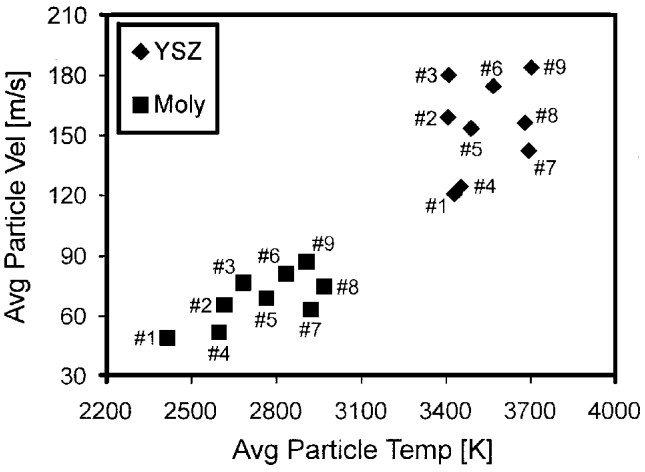

Fig. 8 Ensemble average particle velocity and temperature data at nine sets of torch parameters selected using the torch energy balance

3.2 Particle Velocity and Temperature Measurements

Commercial YSZ (Praxair AI-1075) and molybdenum (Praxair Mo-102) thermal spray powders were used in the ex-

Table 2 Bulk Properties for YSZ and Molybdenum and Spray Particle Size Data

Material	T_m (K)	ρ (kg/m^3)	k (W/mK)	C_p (kJ/kgK)	$D_{v,50}$ (μm)	$D_{[1,0]}$ (μm)
YSZ	2950 (a)	5 890 (a)	2.4 (b)	0.604 (c)	43.1	13.5
Molybdenum (d)	2883	10 280	139	0.260	58.8	38.9

(a) From Ref. 5.
(b) From Ref. 31.
(c) From Ref. 32.
(d) Properties at 298 K from Ref. 33.

periments. Bulk properties for these materials are listed in Table 2. Mass median ($D_{v,50}$) and ensemble average ($D_{[1,0]}$) particle diameters were obtained by sonic sifting.[29] An explanation of these characteristic diameters can be found in Ref. 30. Particle measurements were made between 90 and 100 mm from the torch exit.

Figure 8 presents ensemble-average particle velocity and temperature data for both materials at all nine parameter settings acquired in single spray experiments where all nine torch settings were tested in succession over a short period of time. Each data point represents an average of between 400 and 2500 particles acquired over a period of several seconds. Average particle velocity is plotted against average particle temperature to correspond to Fig. 7, where plasma ρU^2 is plotted against T_g. Comparing the two graphs shows that both spray materials react appropriately to the changes in the plasma conditions at the torch exit.

The YSZ particles track closely with the estimated plasma properties, such that average particle velocity is nearly decoupled from average particle temperature. For molybdenum, however, the average particle velocity is correlated with average particle temperature. Increases in the average particle velocity achieved with a higher plasma ρU^2 are usually accompanied by increases in average particle temperature, even though the plasma temperature is approximately constant. The opposite result is more intuitive, because the faster particles, spending less time in the hot plasma core, ought to end up cooler. However, the reduced residence time may be offset by an increase in the heat transfer rate, which rises in proportion to the particle Reynolds number (Eq 5 and 6).

Particle entrainment effects may also contribute to a positive correlation between particle velocity and temperature. The larger, heavier molybdenum particles have more difficulty becoming entrained into the hot plasma core, particularly when ρU^2 is low, leading to significant spray droop and possibly lower particle temperatures. At larger values of ρU^2, these heavy particles will be better entrained and reach higher temperatures, along with higher velocities. The carrier gas flow rate, which influences particle penetration into the plasma jet,[34] was held constant in the experiments, so that particle entrainment was determined solely by the plasma conditions and the particle characteristics. Better results might have been achieved with molybdenum had the carrier gas flow rate been adjusted for optimum entrainment at each torch setting. The smaller, lighter YSZ particles, being more easily entrained in the plasma jet, may be less susceptible to this coupling effect.

Overall, the experiments demonstrate that the IP-PSV is sensitive to changes in the distribution of particle velocity and temperatures in the spray plume, and thus it should be useful for detecting off-design spray conditions. The data generally agree with particle measurements reported for similar spray materials using more established measurement techniques.[2,4,9,11,12] Exact agreement was not anticipated considering the differences in feedstock material, gas mixtures, and spray equipment used, and the typical uncertainty level associated with two-color pyrometry measurements on thermal spray particles.

3.3 Effectiveness of the Energy Balance Method

The experiments indicate that the energy balance method is a useful approach for controlling plasma spray particles. Figure 9 plots particle velocity against ρU^2 and particle temperature against plasma temperature for repeated experiments conducted over the course of several months. It shows that changes in the average particle velocity and temperature were consistent with the predicted changes in the temperature and dynamic pressure of the plasma jet. Figure 9 also shows the difficulty in reproducing absolute particle temperatures or velocities with the plasma torch, despite nominally identical torch parameters. The average particle temperature varied by up to 100 K in repeat experiments over a period of days, and by several hundred Kelvin in repeat experiments over a period of months, for the same set of torch parameters. Electrode wear, which has been shown to reduce particle temperatures over long periods of spraying even though the net power delivered to the plasma remains fixed,[22] probably causes these seemingly inconsistent results.

Despite the torch consistency problems, the energy balance correctly predicts the response of the average particle characteristics to changes in the torch parameters. This simple, physically based approach may offer advantages as a means to improve the level of control over thermal spray particles compared to computationally intensive numerical simulations[5] or purely empirical techniques.[35] The method can be extended to include more typical plasma gas mixtures, such as Ar-He or Ar-H_2, by using a variable plasma gas composition, provided accurate property data are available for these mixtures. The reliability of plasma property calculations becomes questionable as more components are added, however, because of uncertainties associated with estimating interaction potentials for the multitude of species present in such mixtures.[27] The success of the present experiments suggests that the thermodynamic and transport property data obtained from Ref. 27 for the single-component (argon) plasma used here are relatively reliable.

The apparent control over the average particle velocity and temperature is somewhat less impressive considering that the standard deviations of these properties are as large or larger than the amount by which the averages can be changed. Table 3 lists averages and standard deviations of velocity and temperature for

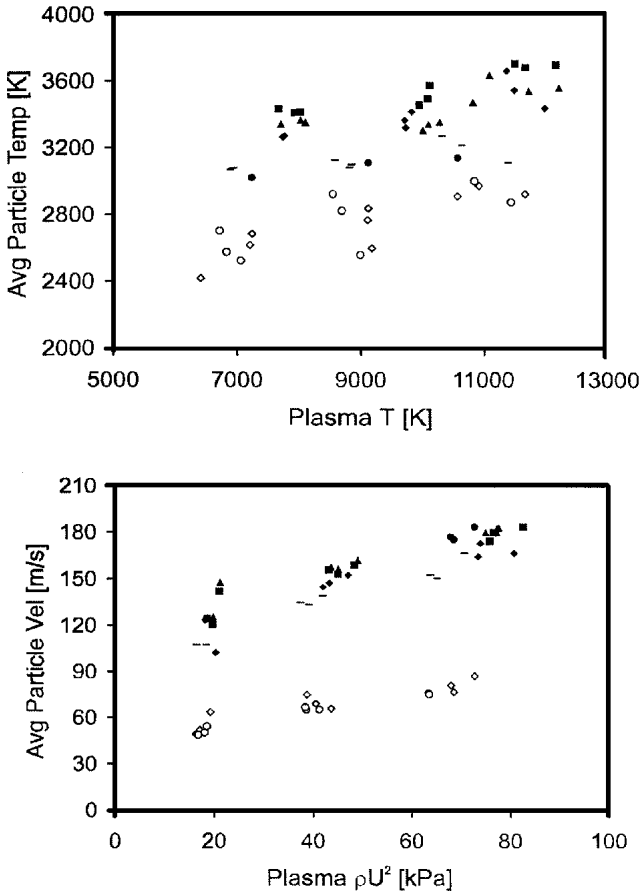

Fig. 9 Correlation between average particle velocity and temperature and predicted plasma properties in repeat experiments. Filled symbols = YSZ; unfilled symbols = molybdenum. Different symbols represent different experiments. In each experiment, measurements were made at each condition in succession without extinguishing the torch.

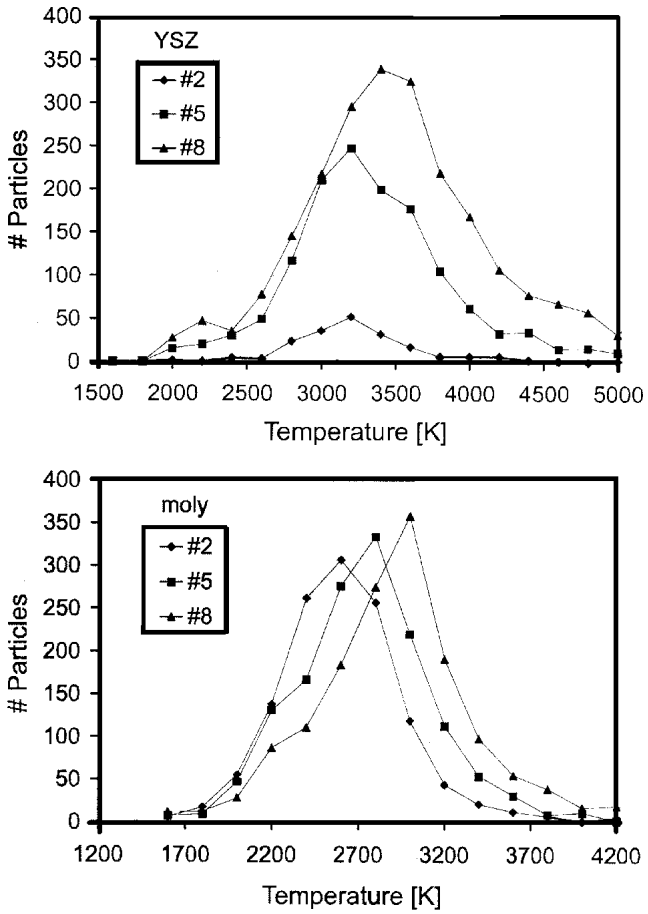

Fig. 10 Temperature histograms for molybdenum and YSZ particles at three gun settings selected to increase temperature and hold velocity constant

Table 3 Typical Averages and Standard Deviations of Particle Velocity and Temperature

Material	Condition	T (K)	σ_T	V (m/s)	σ_v	N/fr (a)
YSZ	2	3260	407	152	26	0.9
	5	3361	582	147	31	5.6
	8	3542	664	145	35	7.6
Molybdenum	2	2616	434	66	12	11.0
	5	2764	511	69	12	12.3
	8	2969	622	75	13	12.3

(a) N/fr = number of particles measured per frame

both powders measured at torch conditions 2, 5, and 8. At these conditions, the plasma temperature is increased while ρU^2 is held nearly constant. Although the average particle temperature increased by 300 K over this range, the standard deviations of particle temperature ranged from 400 K to more than 600 K at the hottest condition. A similar situation exists with particle velocity, though the relevant data are not included in Table 3. Particle temperature histograms are plotted in Fig. 10 for the conditions listed in Table 3. At any torch setting, many particles in the plume are much colder than average, and many are much hotter than average. Overall, the results suggest that although some control over the particle stream is possible, the velocity and temperature of impacting particles that form a thermal spray coating have widely varying properties. This may limit the ability to tightly control coating microstructures. Limiting the number of unmelted particles in the plume appears to be most important because they can seriously degrade coating quality.[37] It should be noted that standard deviations reported for particle temperature using other sensing techniques are smaller by 100 K or more than those reported here.[36] The reason for this difference is presently not understood, but could be caused by some combination of measurement uncertainty in the IP-PSV, differences in dynamic range of the various thermal spray sensors, or the particular operating characteristics of the spray torch used in the present experiments. However, most reported standard deviations are at least 200 K or more, indicating that substantial variability exists in the particle plumes produced by currently available commercial thermal spray torches.

3.4 Time-Resolved Particle Measurements

Many factors contribute to the broad distributions of particle velocity and temperature in plasma spray plumes.[5] One is the

typically wide size range of the powder injected into the plasma jet, because the size of a spray particle affects its acceleration and heating behavior. Radial powder injection may enhance size-based particle segregation, because differently sized particles tend to follow different trajectories, resulting in unique thermal and dynamic histories.[34] Numerical simulations of the spray plume have also estimated the effects of turbulence on particle variability.[5,38] Quasi-periodic fluctuations caused by arc root motion inside the torch also contribute to particle variability.[39] By averaging particles in each successive image, IP-PSV can sense the effect of these instabilities on the particle stream.

In Fig. 11, frame-averaged particle temperature, temperature standard deviation, velocity, and particle flux data are presented for molybdenum at condition 8. The results are generally representative of other spray conditions with both powders. Each data point represents the average of all the particles in a single image normalized by the average of all the particles measured. The average particle temperature and velocity fluctuates by approximately ±10% of the mean value, or about ±300 K in temperature and between ±7 m/s and ±15 m/s in velocity. The standard deviation of particle temperatures and the particle flux vary even more substantially. The magnitude of these fluctuations suggests that plume instabilities indeed play a significant role in creating the wide range of particle velocities and temperatures found in the spray plume.

Because the sensor's frame-rate was limited to 24 Hz, effects due to arc instabilities, which operate at kilohertz frequencies,[39] could not be isolated directly. However, the measurements indicated an instability in the particle stream occurring at about 1 Hz. It is most noticeable in the particle flux plot (Fig. 11, bottom). Powder mass flow measurements made with a coriolis mass flow meter[40] (Micromotion, Boulder, CO) at 10 Hz confirmed that this instability was due to fluctuations in the powder feed to the torch. The ability to detect instabilities in the particle stream may prove useful for evaluating next-generation thermal spray equipment designed for improved spray uniformity.

3.5 Particle Detectability

An important consideration for evaluating a thermal spray particle sensor and interpreting the data it supplies is particle detectability. Particle detectability refers to the minimum amount of thermal radiation that a particle must emit for it to be detected by the sensor. This minimum particle intensity level depends on the optical arrangement, the detector sensitivity, the allowable exposure time, and background signal levels. The brightness of a particle depends on its temperature, size, and emissivity. The velocity and position of the particle within the field of view also affects its intensity signal. Because the intensity signal of a given particle depends on many factors in addition to its temperature, it is difficult to estimate a minimum measurable particle temperature that would be valid for a wide variety of spray materials or conditions. Instead, detection limits must be determined by experiment.

In the present experiments, few YSZ particles were measured below 2000 K, whereas molybdenum particles could be detected down to about 1700 K. The difference in detectability is primarily due to differences in the size and density of these particles. The larger, slower-moving molybdenum particles produce larger intensity signals, allowing lower particle temperatures to be measured. In addition to being smaller and faster, the YSZ particles may also have a lower emissivity, especially if they become translucent at high temperatures.

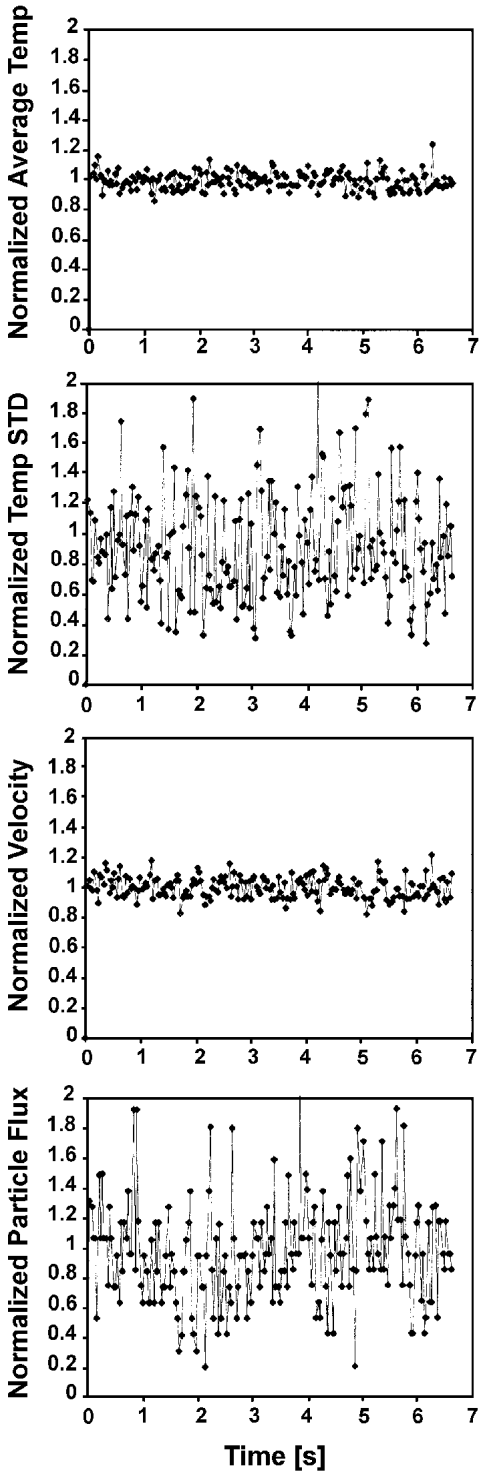

Fig. 11 Frame-averaged particle temperature, temperature standard deviation, velocity, and flux as a function of time for molybdenum at condition 8 normalized by overall average values (see Table 3)

Few results are available in the literature that demonstrate the

practical detectability limits of the various two-color pyrometry techniques on different thermal spray powders. In one study[11] involving a single particle measurement technique, no data were reported below about 2600 K for a commercial YSZ powder, similar to the powder used in the present experiments. Detectability limits of about 1600 K are reported for NiCrAlY and stabilized zirconia powders using another small-volume measurement technique,[36] although no data appear below about 1800 K. However, the spray conditions used in both studies were selected to achieve a high fraction of molten particles because coatings were produced for analysis, and these minimum temperatures may simply have reflected an absence of colder particles in the spray.

Understanding particle detectability is necessary to properly interpret the measurement data, such as estimating the fraction of melted versus unmelted particles in the spray. Unmelted particles contribute to low deposition efficiencies and may become entrapped in the coating and create defects. Alternate sensing techniques that do not depend on thermal emission from particles have been employed to detect cold particles.[37] In the present experiments, the detectability limit for YSZ particles resulted in an obvious discrepancy between measured and expected average particle temperatures when the plasma jet temperature was low (conditions 1-3, Table 1). Although the indicated average particle temperature was above the melting point of YSZ for these conditions, little or no deposition was recorded on a mild steel test substrate, indicating that only a small fraction of the particles were actually molten. At the low temperature conditions, less than one particle was measured per frame on average, compared to six or seven per frame for the hotter conditions, even though the number of particles in the plume remained nominally the same. Thus, a significant number of cold particles escape detection, leading to an overestimate of the average particle temperature. In contrast, when molybdenum particles were sprayed, ample data were recorded at every condition, and low-temperature particles were easier to detect. Better correspondence between the apparent deposition efficiency and the sensor-indicated particle temperature was obtained when spraying molybdenum.

Particle detectability is also important in cases where measurement data are used to validate computational models of the spray plume, or in cases where sensors are used to investigate and optimize the use of new thermal spray powders or processes. Detectability is less important when a sensor is used only to detect unwanted changes in the particle plume in a well-characterized thermal spray operation.[7,8,37] In such cases the sensor need only indicate whether or not the process has drifted beyond an acceptable operating window. Detectability is unimportant as long as it does not interfere with the sensors' ability to accurately identify when the process drifts beyond this specified window.

4. Summary

This paper described calibration experiments and air plasma spray particle measurements using a new particle sensing technique involving two-color IP and PSV. This measurement technique allows particle temperatures and velocities to be measured over a large volume of the spray plume simultaneously. The following items were discussed or concluded:

- The IP-PSV sensor was calibrated to 3,654 K using a unique measurement facility located at the National Institute of Standards and Technology (NIST) in which the absolute temperature and emissivity of the calibration source were measured.
- Particle temperature uncertainties from random sources were estimated at between 1.5% and 4%. An additional systematic temperature error occurs if the particles deviate from graybody behavior.
- The IP-PSV sensor properly detected changes in particle velocity and temperature distributions caused by intentionally altered plasma conditions, and therefore should prove useful as a means to detect unwanted drift in thermal spray processes over extended periods of time.
- The average particle velocity and temperature could be manipulated in desired ways over a wide range using a one-dimensional energy balance model of the plasma torch. This simple physical approach may have advantages as a means of controlling particle behavior over computationally intensive numerical models or purely empirical methods, provided reliable plasma property data are available.
- The IP-PSV measured a 10% fluctuation in average particle velocity and temperature over periods of several seconds. These fluctuations, caused by a combination of arc instabilities, turbulence, and variable powder feed, contribute substantially to the overall variability of particle temperature and velocity in the spray plume.
- Particle detectability must be considered when interpreting particle measurement data obtained from any sensor that measures thermal radiation emitted by particles. Under low power conditions, the indicated average particle temperature can be overestimated because a large number of cold particles escape detection. Particle size, velocity, position, and emissivity affect the detectability of a thermal spray particle.

Acknowledgments

The authors wish to thank R.D. Jiggetts, P.A. Boyer, B. Parke, and R.J. Schaefer of NIST and J. Craig and R. Parker of Stratonics, Inc., for their assistance with this work. The assistance of Praxair Surface Technologies is also gratefully acknowledged.

References

1. P. Gougeon, C. Moreau, and F. Richard: "On-Line Control of Plasma Sprayed Particles in the Aerospace Industry" in *Advances in Thermal Spray Science and Technology*, C.C. Berndt and S. Sampath, ed., ASM International, Materials Park, OH, 1995, pp. 149-55.
2. M. Prystay, P. Gougeon, and C. Moreau: "Correlation between Particle Temperature and Velocity and the Structure of Plasma Sprayed Zirconia Coatings" in *Thermal Spray: Practical Solutions for Engineering Problems*, C.C. Berndt, ed., ASM International, Materials Park, OH, 1996, pp. 517-23.
3. R.N. Wright, J.R. Fincke, W.D. Swank, and D.C. Haggard: "Particle Velocity and Temperature Influences on the Microstructure of Plasma Sprayed Nickel" in *Thermal Spray: Practical Solutions for Engineering Problems*, C.C. Berndt, ed., ASM International, Materials Park, OH, 1996, pp. 511-16.
4. X. Jiang, J. Matejicek, A. Kulkarni, H. Herman, S. Sampath, D.L. Gil-

more, and R.A. Neiser: "Process Maps for Plasma Spray Part II: Deposition and Properties" in *Thermal Spray: Surface Engineering via Applied Research*, C.C. Berndt, ed., ASM International, Materials Park, OH, 2000, pp. 157-63.
5. R.L. Williamson, J.R. Fincke, and C.H. Chang: "A Computational Examination of the Sources of Statistical Variance in Particle Parameters During Thermal Plasma Spraying" in *Thermal Spray: Surface Engineering via Applied Research*, C.C. Berndt, ed., ASM International, Materials Park, OH, 2000, pp. 115-24.
6. J.R. Fincke, W.D. Swank, D.C. Haggard, T.M. Demeny, S.M. Pandit, and A.R. Kashani: "Feedback Control of the Subsonic Plasma Spray Process: System Model" in *Advances in Thermal Spray Science and Technology*, C.C. Berndt and S. Sampath, ed., ASM International, Materials Park, OH, 1995, pp. 117-22.
7. G. Bourque, M. Lamontagne, and C. Moreau: "A New Sensor for On-Line Monitoring the Temperature and Velocity of Thermal Spray Particles" in *Thermal Spray: Surface Engineering via Applied Research*, C.C. Berndt, ed., ASM International, Materials Park, OH, 2000, pp. 45-50.
8. J. Zierhut, K.D. Landes, W. Krömmer, and P. Heinrich: "Particle Flux Imaging (PFI) In-Situ Diagnostics for Thermal Coating Process" in *Thermal Spray: Surface Engineering via Applied Research*, C.C. Berndt, ed., ASM International, Materials Park, OH, 2000, pp. 63-66.
9. J.R. Fincke and W.D. Swank: "Air-Plasma Spraying of Zirconia: Spray Characteristics and Standoff Distance Effect on Deposition Efficiency and Porosity" in *Thermal Spray: International Advances in Coatings Technology*, C.C. Berndt, ed., ASM International, Materials Park, OH, 1992, pp. 513-18.
10. C.M. Hackett and G.S. Settles: "Independent Control of HVOF Particle Velocity and Temperature" in *Thermal Spray: Practical Solutions for Engineering Problems*, C.C. Berndt, ed., ASM International, Materials Park, OH, 1996, pp. 665-73.
11. B.M. Cetegen and W. Yu: "In-Situ Particle Temperature, Velocity, and Size Measurements in DC Arc Plasma Thermal Sprays," *J. Thermal Spray Technol*., 1999, *8*(1), pp. 57-67.
12. K. Hollis and R. Neiser: "Particle Temperature and Flux Measurement Utilizing a Nonthermal Signal Correction Process," *J. Thermal Spray Technol*., 1998, *7*(3), pp. 392-402.
13. J.R. Fincke, C.L. Jeffery, and S.B. Englert, "In-Flight Measurement of Particle Size and Temperature," *J. Phys. E: Sci. Instrum.*, 1988, *21*, pp. 367-70.
14. J.E. Craig, R.A. Parker, D.Y. Lee, F.S. Biancaniello, and S.D. Ridder: "A Two-Wavelength Imaging Pyrometer for Measuring Particle Temperature, Velocity and Size in Thermal Spray Processes" in *Proceedings of the International Symposium on Advanced Sensors for Metal Processing*, Industrial Materials Institute, NRC Canada, 1999, pp. 369-80.
15. J.E. Craig, R.A. Parker, D.Y. Lee, F.S. Biancaniello, S.D. Ridder, and S.P. Mates: "Particle Temperature Measurements by Spectroscopic and Two-Wavelength Streak Imaging" in *Thermal Spray: Surface Engineering via Applied Research*, C.C. Berndt, ed., ASM International, Materials Park, OH, 2000, pp. 51-56.
16. A. Cezairliyan, "Design and Operational Characteristics of a High-Speed (Millisecond) System for the Measurement of Thermophysical Properties at High Temperatures," *J. Res. Nat. Bur. Stand. (U.S.)*, 1971, *75C*(1), p. 7.
17. A. Cezairliyan, S. Krishnan, and J.L. McClure: "Simultaneous Measurements of Normal Spectral Emissivity by Spectral Radiometry and Laser Polarimetry at High Temperatures in Millisecond-Resolution Pulse-Heating Experiments: Application to Molybdenum and Tungsten," *Int. J. Thermophys.*, 1996, *17*(6), pp. 1455-73.
18. D. Basak, U.R. Kattner, J.L. McClure, D. Josell, and A. Cezairliyan: "Application of Laser Polarimetry to the Measurement of Specific Heat Capacity and Enthalpy of the Alloy 53Nb-47Ti (Mass%) in the Temperature Range 1600 to 2000 K by a Millisecond-Resolution Pulse Heating Technique," *Int. J. Thermophys.*, 2000, *21*(4), pp. 913-26.
19. D.P. Dewitt and G.D. Nutter: *Theory and Practice of Radiation Thermometry*, John Wiley-Interscience, New York, 1988.
20. F.A. Graybill and H.K. Iyer: *Regression Analysis: Concepts and Applications*, Duxbury Press, Belmont, CA, 1994.
21. P. Gougeon and C. Moreau: "In-Flight Particle Surface Temperature Measurement: Influence of the Plasma Light Scattered by the Particles" in *Thermal Spray Coatings: Research, Design and Applications*, C.C. Berndt and T.F. Bernecki, ed., ASM International, Materials Park, OH, 1993, pp. 13-18.
22. L. Leblanc and C. Moreau: "Study on the Long-Term Stability of Plasma Spraying" in *Thermal Spray: Surface Engineering via Applied Research*, C.C. Berndt, ed., ASM International, Materials Park, OH, 2000, pp. 1233-39.
23. E. Pfender: "Heat and Momentum Transfer to Particles in Thermal Plasma Flows," *Pure Appl. Chem.*, 1985, *57*(9), pp. 1179-95.
24. C.M. Hackett, G.S. Settles, and J.D. Miller: "On the Gas Dynamics of HVOF Thermal Sprays," *J. Thermal Spray Technol.*, 1994, *3*(3), pp. 299-304.
25. E. Pfender: "Plasma Jet Behavior and Modeling Associated with the Plasma Spray Process," *Thin Solid Films*, 1994, *238*, pp. 228-41.
26. C.H. Chang and J.D. Ramshaw: "Modeling of Non-Equilibrium Effects in a High-Velocity Nitrogen-Hydrogen Plasma Jet," *Plasma Chem. Plasma Process.*, 1996, *16*, pp. 5S-17S.
27. M.I. Boulos, P. Fauchais, and E. Pfender: *Thermal Plasmas, Fundamentals and Applications*, Vol. 1, Plenum, New York, 1994.
28. A. Vardelle, P. Fauchais, B. Dussoubs, and N.J. Themelis: "Heat Generation and Particle Injection in a Thermal Plasma Torch," *Plasma Chem. Plasma Process.*, 1998, *18*(4), pp. 551-74.
29. F.S. Biancaniello, J.J. Conway, P.I. Espina, G.E. Mattingly, and S.D. Ridder: "Particle Size Measurement of Inert-Gas-Atomized Powder," *Mater. Sci. Eng*., 1990, *A124*, pp. 9-14.
30. A.H. Lefevbre: *Atomization and Sprays*, Hemisphere, New York, 1989.
31. D.P.H. Hasselman, L.F. Johnson, L.D. Bentsen, R. Syed, H.L. Lee, and M.V. Swain: "Thermal Diffusivity and Conductivity of Dense Polycrystalline ZrO_2 Ceramics: A Survey," *Am. Ceram. Soc. Bull.*, 1987, *66*(5), pp. 799-806.
32. M. Vardelle, A. Vardelle, A.C. Leger, P. Fauchais, and D. Gobin: "Influence of Particle Parameters at Impact on Splat Formation and Solidification in Plasma Spraying Processes," *J. Thermal Spray Technol*., 1995, *4*(1), pp. 50-58.
33. F.M. White: *Heat and Mass Transfer*, Addison-Wesley, New York, 1991.
34. M. Vardelle, A. Vardelle, B. Dussoubs, P. Fauchais, T.J. Roemer, R.A. Neiser, and M.F. Smith: "Influence of Injector Geometry on Particle Trajectories: Analysis of Particle Dynamics in the Injector and Plasma Jet" in *Thermal Spray: Meeting the Challenges of the 21st Century*, C. Coddet, ed., ASM International, Materials Park, OH, 1998, pp. 887-94.
35. D.L. Gilmore, R.A. Neiser, Y. Wan, and S. Sampath: "Process Maps for Plasma Spray Part I: Plasma-Particle Interactions" in *Thermal Spray: Surface Engineering via Applied Research*, C.C. Berndt, ed., ASM International, Materials Park, OH, 2000, pp. 149-55.
36. J.R. Fincke, R.L. Williamson, and C.H. Chang: "Plasma Spraying of Functionally Graded Materials: Measured and Simulated Results" in *Thermal Spray: Surface Engineering via Applied Research*, C.C. Berndt, ed., ASM International, Materials Park, OH, 2000, pp. 141-48.
37. J.R. Fincke and R.A. Neiser: "Advanced Diagnostics and Modeling of Spray Processes," *MRS Bulletin*, Materials Research Society, 2000, *25*(7), pp. 26-31.
38. I. Ahmed and T.L. Bergman: "Three-Dimensional Simulation of Thermal Plasma Spraying of Partially Molten Ceramic Agglomerates," *J. Thermal Spray Technol*., 2000, *9*(2), pp. 215-24.
39. Z. Duan, L. Beall, J. Schein, J. Heberlein, and M. Stachowicz: "Diagnostics and Modeling of an Argon/Helium Plasma Spray Process," *J. Thermal Spray Technol*., 2000, *9*(2), pp. 225-34.
40. J.T. Walker, "Advances in Coriolis Technology for Precision Flow and Density Measurements of Industrial Fluids" in *Proceedings of the Annual Symposium on Instrumentation for the Process Industries*, Texas A&M University, College Station, TX, 1992, pp. 69-73.